Electronic excitations in shocked nitromethane

Evan J. Reed* and J. D. Joannopoulos
Department of Physics, Massachusetts Institute of Technology, Cambridge, Massachusetts 02139

Laurence E. Fried
Chemistry and Materials Science Directorate, Lawrence Livermore National Laboratory, Livermore, California 94550
(Received 9 August 2000)

The nature of electronic excitations in crystalline solid nitromethane under conditions of shock loading and static compression are examined. Density-functional theory calculations are used to determine the crystal bandgap under hydrostatic stress, uniaxial strain, and shear strain. Bandgap lowering under uniaxial strain due to molecular defects and vacancies is considered. *Ab initio* molecular-dynamics simulations are done of all possible nearest-neighbor collisions at a shock front, and of crystal shearing along a sterically hindered slip plane. In all cases, the bandgap is not lowered enough to produce a significant population of excited states in the crystal. The nearly free rotation of the nitromethane methyl group and localized nature of the highest occupied molecular orbital and lowest unoccupied molecular orbital states play a role in this result. Dynamical effects have a more significant effect on the bandgap than static effects, but relative molecule velocities in excess of 6 km/s are required to produce a significant thermal population of excited states.

I. INTRODUCTION

The last two decades have produced significant new insights into the basic science of high explosives. Experiments and theory have suggested that the sensitivity of high explosives to initiation by mechanical perturbations or shocks is a strong function of solid-state properties including crystal structure, defects, and dislocations.[1–5] Behind a shock front lies a region that is far from equilibrium, where solid-state properties may determine the rates and mechanisms through which the material reaches equilibrium.

Any complete microscopic description of the initiation of high explosives will elucidate the mechanisms of energy transfer into the individual molecules from a shock wave.[6] No such theory currently exists in a widely agreed upon form.

One possible energy transfer mechanism involves shock-wave-induced electronic excitations of the molecules. In 1971, Williams suggested that excited states play a role in the initiation and propagation of detonation waves in explosives.[7] A similarity between shock decomposition products to those of photochemical processes was later pointed out by Dremin *et al.*[8] A correlation has been reported between the impact sensitivity of a homologous series of explosives and the energies of their optically forbidden electronic transitions across the bandgap.[9] Gilman has proposed metallization at the shock front resulting from bending of covalent bonds.[10] Such metallization has been found to occur under static pressure conditions in the covalently bonded crystalline semiconductors Si and Ge. These materials undergo a phase transition to a metallic phase at pressures comparable to those found in detonating energetic materials.[11] Finally, Kuklja *et al.*, have proposed bandgap lowering and electronic excitations around crystal defects under compression as a mechanism for detonation initiation.[12]

Chemistry is thought to begin to occur on a 10 or 100 ps time scale behind a shock front in some energetic materials.[1] This requires a fast mechanism of energy transfer from the shock wave to the molecular degrees of freedom. A mechanism for energy transfer from the shock directly into molecular electronic degrees of freedom is appealing because electronic excitation to an unstable energy surface can result in rapid dissociation of a molecule. A similar mechanism has been found to be a cause of rapid migration of interstitials in crystalline silicon subjected to radiation.[13]

Manaa *et al.*, have done *ab initio* complete active space self-consistent field studies of molecular nitromethane (CH_3NO_2).[14] They found that the highest occupied molecular orbital (HOMO) and lowest unoccupied molecular orbital (LUMO) states can be made to cross by bending the nitro group out of the CNOO plane by approximately 50 degrees. This is the lowest energy HOMO-LUMO crossing point. This molecular geometry is similar to the triplet (excited) state geometry, which lies 0.6 eV below in energy. These results suggest that nonradiative transitions from the excited state to a vibrationally hot ground state may be possible.

In this work we examine mechanisms of electronic excitations by a shock wave in solid nitromethane. Nitromethane is one of the simplest model energetic materials, and is an analog of commonly used energetic materials such as TATB (1,3,5-triamino-2,4,6-trinitrobenzene) and TNT (2,4,6 trinitrotoluene). Here, we study the effect of the various conditions found in a shock or detonation wave on the bandgap of the solid.

II. COMPUTATIONAL DETAILS

Density-functional theory calculations were performed using the PW91 (Ref. 15) and PBE (Ref. 16) generalized-gradient approximations (GGA's) of Perdew. These exchange-correlation functionals produced nearly identical results in comparison cases. Calculations utilized Troullier-Martins pseudopotentials[17] and Vanderbilt ultrasoft pseudopotentials.[18] Plane waves with kinetic energy cutoffs

of 25 and 40 Ry were used with the Vanderbilt and Troullier-Martins pseudopotentials, respectively. Results obtained using the two sets of pseudopotentials are in good agreement. All calculations were converged with respect to *k*-point spacing in the Brillouin zone. In many cases, a single *k* point was sufficient due to the minimal amount of dispersion across the single-particle bands. Stresses reported here were calculated using an analytic approach based on plane-wave basis functions.[19]

Nitromethane is in the liquid state at room temperature and pressure, but most practical energetic materials are in a solid state under these conditions. We have chosen to study the crystalline form of nitromethane in analogy with other energetic materials. The primitive cell of nitromethane at zero pressure contains four molecules. Figure 1 contains three projections onto the lattice planes, and the left side of Fig. 2 contains a perspective view. The atomic positions have been relaxed within the experimental lattice parameters. The space group is $P2_12_12_1$ with orthorhombic lattice vectors $a=5.1832$ Å, $b=6.2357$ Å, and $c=8.5181$ Å at $T=4.2$ K.[20] Adjacent molecules along the *c* axis have alternating nitro and methyl groups which gives the unit cell a neutral overall dipole moment. Rotation of the methyl group has a very low barrier of about 118 K.[21] It is therefore essentially a free rotor at higher temperatures. The molecular lattice is similar to a face-centered structure, with each molecule having 12 nearest-neighbor molecules. The atomic positions and bond lengths of the relaxed structure at the experimental lattice size were found to be within 3% of the experimentally determined positions and bond lengths at $T=4.2$ K.[20] Unless otherwise noted, all atoms in the unit cell were relaxed in the calculations presented here.

The calculated bandgap for the crystal at zero pressure is 3.28 eV. The HOMO-LUMO gap for a single molecule is 3.75 eV. This is similar to the 3.8 eV HOMO-LUMO gap for a single molecule calculated using multiconfiguration self-consistent field (MCSCF) techniques by Manaa and Fried.[22] Electron-impact spectroscopy techniques have been used to measure this transition for molecular nitromethane.[23] The intensity was observed to have an onset at 3.1 eV and a maximum intensity at 3.8 eV. We find that the relatively weak intermolecular interactions in the solid phase cause the bandgap to differ from the isolated molecule HOMO-LUMO energy difference only slightly.

The error associated with the bandgaps presented here is roughly estimated to be around 0.5 eV. Bandgaps calculated for unit cells relaxed within the local-density approximation (LDA) for exchange and correlation energy were all within 0.3 eV of the GGA values presented here. While bandgaps calculated within the LDA are typically a factor of 2 less than experimental values,[24] we believe the gaps presented here to be more accurate for the following reason. One of the assumptions associated with density-functional theory (DFT) quasiparticle energies is that removal or addition of a particle to a state leaves the total density unchanged.[24] The HOMO and LUMO states of a nitromethane molecule are both localized to the atoms in the nitro group, which results in a relatively minor change in the total density when an electron is transferred from the HOMO to the LUMO. Therefore, the other occupied states do not require significant adjustments since the Kohn-Sham Hamiltonian is a functional only of the total density. Indeed the calculated HOMO-LUMO gap for a single molecule is almost identical to the experimental value. We expect to observe a similar behavior for the crystal bandgap. The nitromethane solid bandgap has been calculated within density-functional theory using a bandgap correction based on the above idea.[24] The difference between the corrected and uncorrected bandgaps was found to be only 0.2 eV.[25] Manaa and Fried also report good agreement between DFT and complete active space self-consistent field methods for molecular nitromethane excited state energies.[14]

If, upon compression or molecular distortion, the molecu-

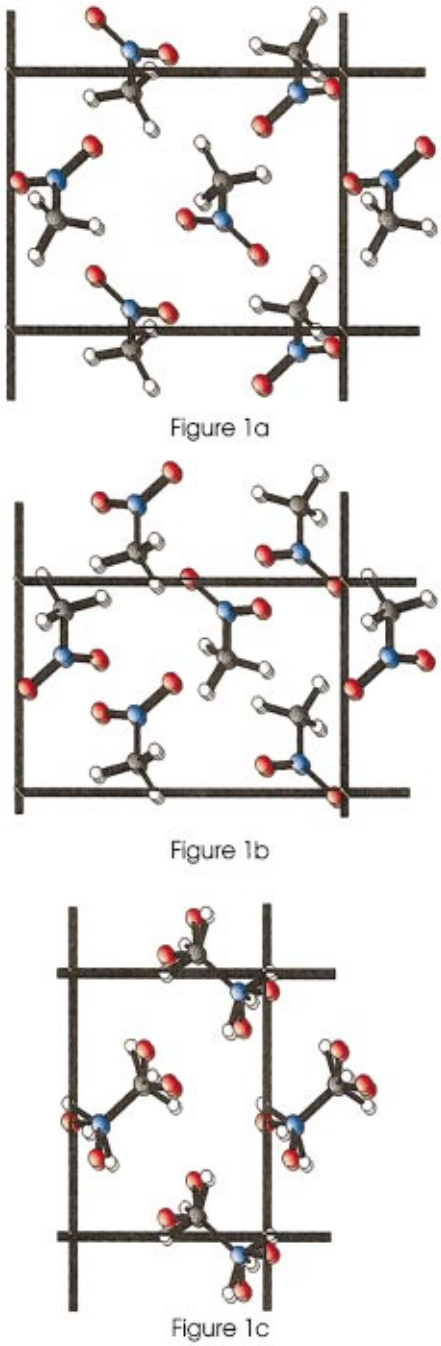

FIG. 1. (Color) Three projections of nitromethane unit cell at zero pressure and zero temperature on, (a) the *zy* plane; (b) the *zx* plane; (c) the *xy* plane. Hydrogen atoms are white, carbons atoms are gray, nitrogen atoms are blue, and oxygen atoms are red.

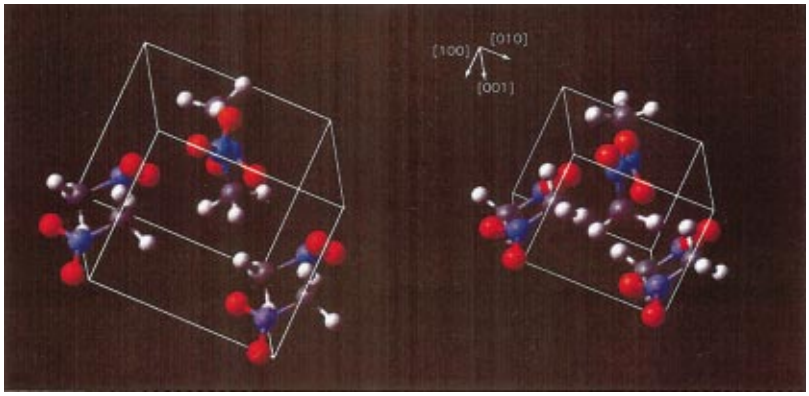

FIG. 2. (Color) Comparison of the unit cell at zero (left) and 180 GPa (right) hydrostatic pressure. (Comparison is approximately to scale.) The orientation of the molecules is roughly the same at the two pressures, except for a significant rotation of the methyl group.

lar orbitals rearrange such that the HOMO state density is no longer similar to the LUMO state density, we would expect to see an artificial lowering in the bandgap analogous to that seen in semiconductor systems. However, we also expect the dielectric screening to increase as the system density increases. This will reduce the significance of nonlocal many-body effects neglected in the exchange-correlation energy approximation used here. These effects lead us to expect our calculated bandgaps to be equal to or less than the true bandgaps.

This has been demonstrated in more accurate quasiparticle calculations on solid xenon[26] within the GW approximation of Hybertson and Louie.[27] LDA bandgaps were shown to underestimate the experimental and GW approximation bandgaps at all densities up to metallization. Furthermore, the difference between the LDA bandgap and the GW and experimental bandgaps diminished as the density increased. This effect was attributed to the increase of dielectric screening at higher densities.

As another preliminary check on the theoretical approximations employed, the molecular vibrational frequencies were computed by calculating the molecular Hessian and then diagonalizing the dynamical matrix. All vibrational frequencies were found to be within 5% of experimental values with the exception of the very high-frequency CH symmetric stretch modes. These frequencies were up to 9% higher than experimental values. Tuckerman *et al.*, also found good agreement between experimental and calculated nitromethane vibrational spectra using techniques similar to ours.[37]

III. STATIC CONDITIONS

A. Hydrostatic compression

In regions sufficiently far behind the shock front for the stress tensor to be equilibrated, a condition of hydrostatic compression exists. Starting at the experimental atmospheric pressure lattice size, the unit cell was compressed up to a hydrostatic pressure of 180 GPa with 6 intermediate pressure points. At each pressure, the lattice vectors and atoms in the unit cell were relaxed according to the forces. Table I contains the calculated lattice vectors at the pressures considered here. There is a lack of experimental lattice constant data at these higher pressures, but we expect the agreement between experiment and DFT to improve as the pressure increases the strength of the intermolecular interactions.

In the pressure range explored, the crystal structure maintained the $P2_12_12_1$ symmetry. No bond bending was observed, but the 180 GPa molecules have bond lengths shortened by 7–15 %. A phase transition of the methyl group rotation angle was observed to occur between the 10 and 30 GPa calculations. Such a transformation has been observed experimentally at 3.5 GPa.[28] It is possible that the zero-pressure orientation of the hydrogens is only metastable in the 10 GPa calculation. There is also experimental evidence for a structural phase transition at 7 GPa at higher temperatures,[29] but a spontaneous phase transition was not observed in the calculations. The $P2_12_12_1$ structure is at least metastable in this pressure range at zero temperature. Cortecuisse *et al.*, have speculated that the phase transition at 7 GPa is associated with an increase in the number of molecules in the unit cell. A unit cell of eight molecules with the *a* axis doubled and relaxed at 30 GPa was also found to be at least metastable.

Figures 2 and 3 contain the unit-cell configurations and band structures at 2 and 180 GPa. The bands at low pressure are relatively flat compared to high pressure where dispersion plays a role. As the pressure increases, band dispersion first appears in the midvalence range, leaving the HOMO state relatively flat. This result is most likely associated with the extended nature of the states in this range. These states are delocalized over the whole molecule, while the HOMO state is localized on the nitro group. Intermolecular interactions should have a greater effect on orbitals that extend over the entire molecule, since they have larger overlaps than localized orbitals.

The bandgap change as a function of pressure is given in Fig. 4. The HOMO-LUMO gap of a single molecule in the geometry of the 180 GPa calculation was found to be 3.96 eV using MCSCF techniques.[30] This indicates that condensed phase effects are important in producing the band gap reduction as a function of pressure. The detonation pressure and temperature of nitromethane has been experimentally de-

TABLE I. Nitromethane lattice constants, in Ångstroms, calculated at various pressures.

	Hydrostatic pressure (GPa)							
	2	10	30	60	90	120	150	180
a	5.183	4.496	4.174	3.998	3.878	3.802	3.725	3.674
b	6.235	5.772	5.199	4.925	4.745	4.615	4.522	4.448
c	8.518	8.211	7.476	7.090	6.852	6.621	6.496	6.353

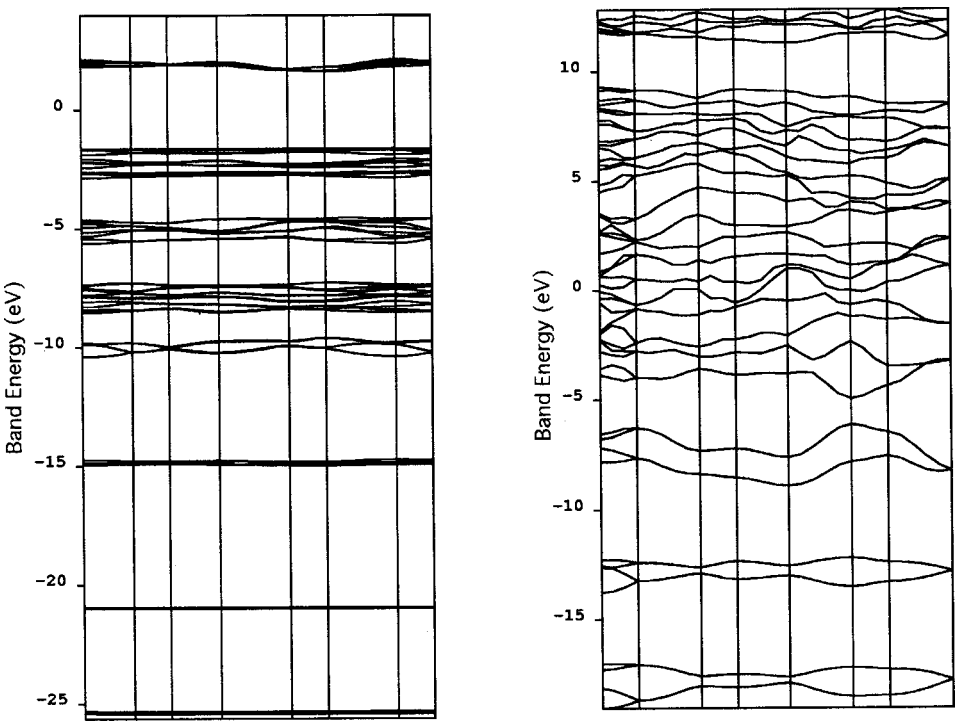

FIG. 3. Comparison of single-particle band structures at zero (left) and 180 GPa (right) hydrostatic pressure. The top four bands are conduction bands.

termined to be about 13 GPa and 2000 K, respectively,[31] and there is not a significant change in the bandgap in the vicinity of this pressure. Even compressing the crystal to a pressure an order of magnitude higher than that observed in developed detonation waves results in a bandgap lowering to around 2 eV, which is not sufficiently low to provide a significant thermal conduction band population at the observed temperatures.

These results are qualitatively comparable to those of other theoretical studies. Hartree-Fock calculations have been performed by Younk and Kunz on RDX (hexahydro-1,3,5-trinitro-s-trizine), lithium azide (LiN_3), sodium azide (NaN_3), and lead azide $Pb(N_3)_2$.[12,32] Upon compression to densities associated with detonation, most of these materials also showed some bandgap lowering, but not enough to produce a significant population of excited states at temperatures associated with detonation.

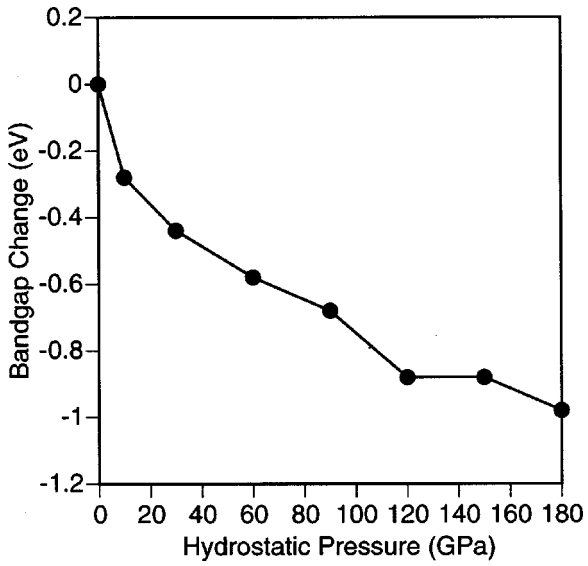

FIG. 4. Nitromethane bandgap change as a function of hydrostatic pressure. Bandgaps are plotted relative to the zero-pressure state.

B. Uniaxial compression

Before the crystal relaxes to a state of hydrostatic stress, a state of uniaxial strain exists immediately after the shock front passes. This uniaxial strain state may last for picoseconds or much longer, depending on the timescale for plastic deformation. The relaxation from this strain state may involve shearing along crystal slip planes or shear wave propagation.

The unit cell at zero pressure was uniaxially strained along each of the three lattice vectors and the molecules within the cell were relaxed at each strain state. Uniaxial strain destroys the $P2_12_12_1$ symmetry in cases of extreme strain. Figure 5 shows the relaxed unit cell upon strain of 0.3 along the *c* axis. There is no significant distortion of the molecular bond angles, although the molecules have reoriented. The molecules are reoriented so that the nitro groups are closer to being in the *ab* plane than they are in the unstrained state. Figure 6 shows the stress in the direction of compression for each of the three compression axes.

Figure 7 shows the bandgap change as a function of compression along each of the three lattice axes. There does not appear to be any significant orientational dependence as a function of the strain axis. With the uniaxial strains associated with detonation around 0.2, the bandgaps are lowered to 3 eV. As in hydrostatic compression, this lowering is not enough to allow a significant thermal population of conduction electrons.

If we move closer to the shock front, the molecules have insufficient time to reorient to relax under the uniaxial strain. Shock compression without relaxation can be modeled by

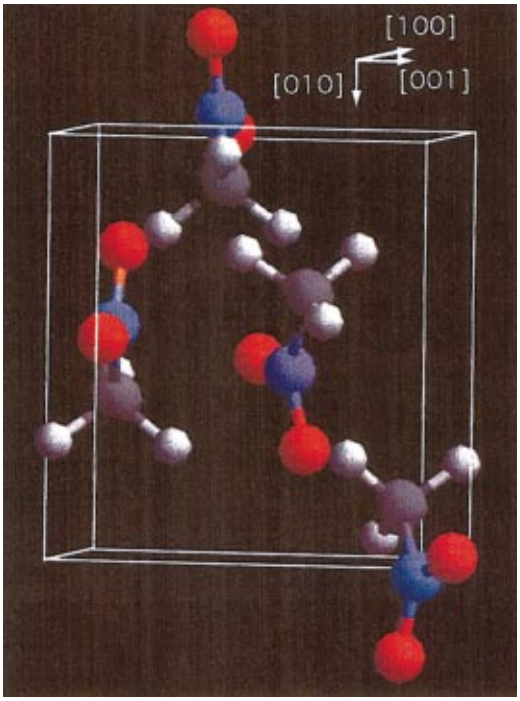

FIG. 5. (Color) Nitromethane unit cell relaxed under a uniaxial strain of 0.35 (3.0 Å) along the *c*-axis direction.

simply translating the molecules toward each other in the direction of uniaxial compression. This simplistic approach is intended to capture some of the dynamics of the compression in a static calculation.

Figure 8 shows the bandgap change as a function of compression without relaxation along each of the three lattice axes. The data indicate an orientational dependence, with the largest bandgap lowering occurring for compression along the *c* axis. Compression along this axis brings the nitro groups closer to methyl groups of neighboring molecules. In particular, it brings a hydrogen on one molecule directly toward an oxygen on a neighboring molecule. Compression

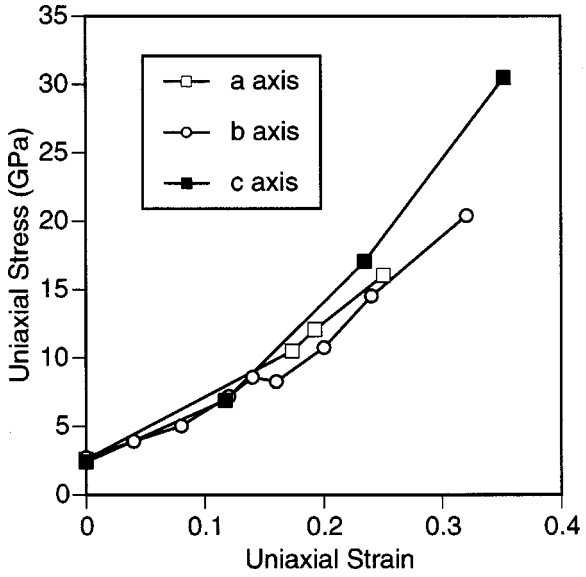

FIG. 6. Nitromethane uniaxial stress in the direction of uniaxial compression.

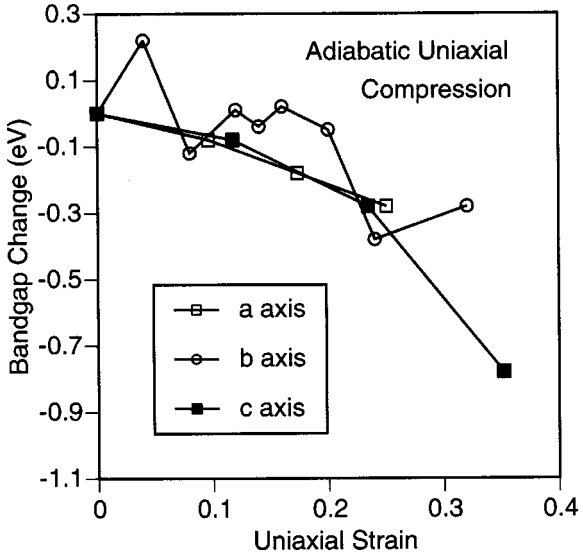

FIG. 7. Nitromethane bandgap change as a function of uniaxial strain. Bandgaps are plotted relative to the unstrained state.

along the other directions does not bring close contact atoms on neighboring molecules directly towards each other. We expect this transient effect to be very short lived because the energy barrier for methyl rotation is only 170 K at atmospheric pressure. The methyl groups will quickly rotate to avoid such a close contact between two atoms. This effect will be addressed in more detail in the section on dynamical effects. It is interesting to note that the *a* axis is a nearest-neighbor direction while the *b* axis is not, yet the bandgap behavior as a function of compression is nearly identical for these two axes. This is likely due in part to the localization of the HOMO and LUMO states to the nitro group.

A similar increased gap lowering for compression of molecules without relaxation was observed by Kuklja, Stefanovich, and Kunz.[33] Without allowing the structure geometry to relax, RDX molecules were placed in a configuration resem-

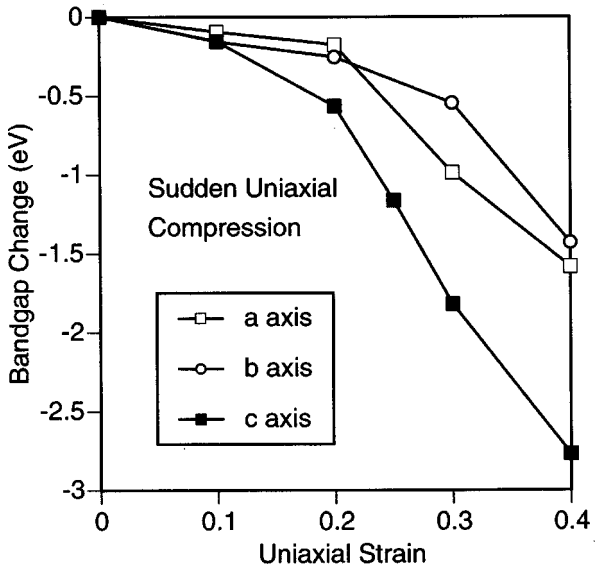

FIG. 8. Nitromethane bandgap change as a function of uniaxial strain without unit cell relaxation. Bandgaps are plotted relative to the unstrained state.

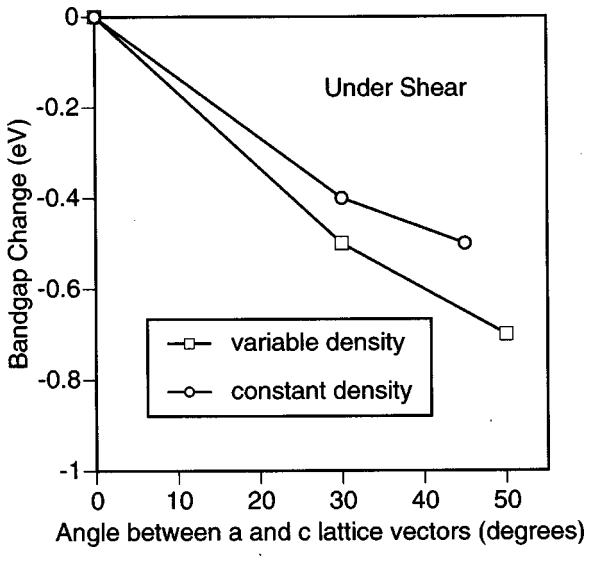

FIG. 9. Nitromethane bandgap change as a function of unit cell shear. Bandgaps are plotted relative to the unstrained state. The angle between the *a* and *c* lattice vectors (γ) was varied. In one data set, the *c* lattice vector length was fixed at all angles. In the other set, the length was varied to keep a constant density at each angle.

bling an edge dislocation. The bandgaps for the compressed and uncompressed structures were considerably lower than those for other model defect structures where molecules had been simply removed from the perfect crystal lattice. The removal of molecules from the relaxed lattice can be accomplished without creating close intermolecular contacts. However, we have observed here that relaxation of the lattice is very important to obtain a reliable bandgap for any other molecular configuration. A comparison of Figs. 7 and 8 demonstrates this.

C. Shear

Strong positive correlations between the impact sensitivity and population of vacancies and defects in high explosive suggest that vacancies and defects play a key role in high explosive initiation. A state of shear strain may exist around defects or along slip planes as a result of the uniaxial compression that occurs at the shock front.

A static state of shear strain was modeled by varying the angle between the *a* and *c* lattice vectors (γ). This was done in two fashions: while keeping the lattice vector lengths fixed, and while adjusting the *c* vector length to keep the cell volume constant (constant density). A third state of shear was considered where the *a* lattice vector was increased while the *c* lattice vector was decreased such that the density remained constant. The results of these calculations are similar to those presented here.

Figure 9 shows the bandgap change as a function of γ for the variable and fixed density cases. Very little gap lowering results from the shearing in both cases. As in the hydrostatic compression and uniaxial compression, the molecules rearrange themselves but exhibit little geometric distortion.

D. Molecular defect

It has been suggested that defects in molecular crystals are sites where increased gap lowering can occur under

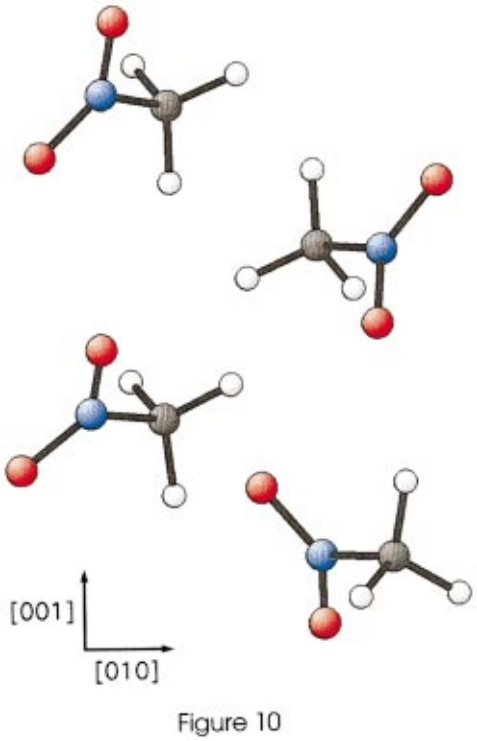

FIG. 10. (Color) Nitromethane unit-cell molecules with a flipped molecule defect. There is an infinite row of molecules along the [001] axis oriented in approximately the same fashion.

pressure.[33] We consider, as a simple defect, a flipped molecule in the unit cell, as shown in Fig. 10. The motivation for this defect is to increase the interactions between HOMO and LUMO states of the flipped molecule and HOMO and LUMO states of a neighboring molecule by bringing them closer together. In this defect configuration, the periodic boundary conditions create an infinite row of molecules along the *c* axis direction with neighboring nitro groups.

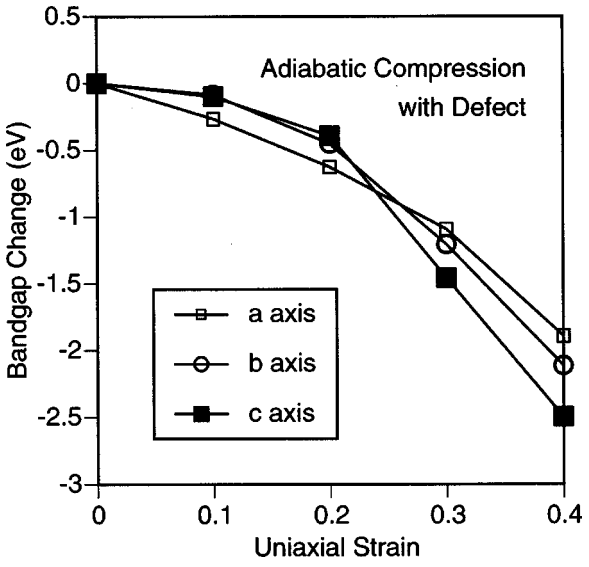

FIG. 11. Nitromethane bandgap change for a unit cell with a molecular defect as a function of uniaxial strain. Bandgaps are plotted relative to the unstrained state, which has a bandgap about 0.5 eV lower that the perfect crystal in its unstrained state.

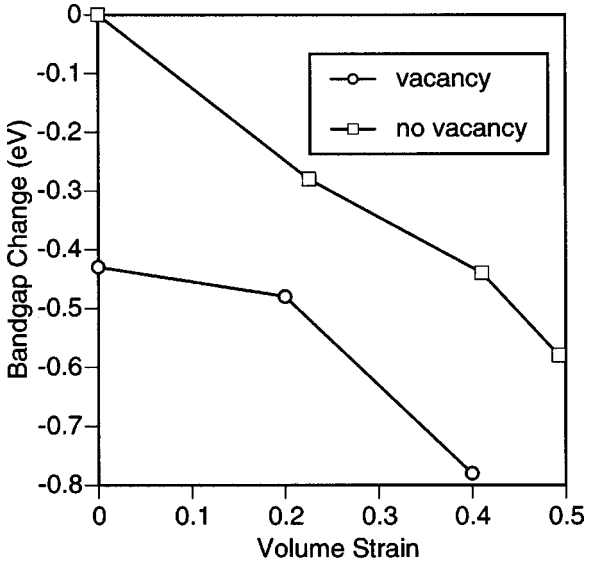

FIG. 12. Nitromethane bandgap change for a unit cell with and without a molecular vacancy as a function of volume strain. Bandgaps are plotted relative to the unstrained states for each system.

This structure was compressed uniaxially and relaxed, with bandgap change results in Fig. 11. The molecular geometries upon compression are within 2–3 % percent of the zero-pressure values, with little or no bond distortion. The bandgap for the unstrained unit cell is about 3.0 eV which is 0.5 eV lower than that of the perfect crystal. The bandgap decreases more quickly with uniaxial strain than it does for the perfect crystal, particularly at high strains. However, the bandgap still does not lower enough to produce a significant population of molecular excited states under conditions of detonation.

E. Molecular vacancy

Another type of lattice defect is a missing molecule. We have simulated such a defect by removing a single molecule from a 16 molecule supercell. Periodic copies of the vacancy are separated by about 9 Å in the unstrained configuration.

Relaxation of the vacancy in the unstrained lattice resulted in almost no distortion from the unperturbed lattice. The bandgap for the relaxed vacancy in the unstrained supercell was lowered about 0.4 eV from the perfect crystal bandgap. This result is on the scale of the energy difference between the perfect crystal bandgap and the HOMO-LUMO gap of an isolated molecule, which is due entirely to intermolecular interactions.

The supercell was strained to 80 and 60 % of the unstrained volume by straining all three lattice vectors the same amount. The relaxed structures showed some molecular reorientation around the vacancy. However, all molecules showed little displacement from their perfect crystal locations.

Figure 12 is a comparison of the bandgaps for the system with and without the molecular vacancy as a function of volume strain. The vacancy provides room for molecules to reorient to avoid bandgap-lowering close contacts. For this reason we might expect the bandgap to decrease less quickly with strain than for systems without a molecular vacancy.

These results are notably different from the results of Kuklja, Stefanovich, and Kunz who have done Hartree-Fock calculations on RDX crystals with various configurations of molecular vacancies.[33] Bandgaps calculated with a form of perturbation theory correction decreased around 2 eV upon compression of the crystal to 80% of the unstrained volume. We may speculate that, in addition to comparing different materials, the different behavior may be due to the fact that relaxation of the molecular positions and geometries was allowed in the work here, in addition to the use of a different theoretical approach to the bandgaps.

We can qualitatively summarize the results of all of the static calculations presented here with two points. The bandgap is not lowered enough to create significant thermal populations of excited states under static conditions with strain states comparable to or greater than those of detonation. Also, upon compression and relaxation, the molecules find a way to rearrange to maintain molecular geometries close to their zero-pressure values. These two points suggest that if significant bandgap lowering is to occur, molecular bond distortion is required.

IV. DYNAMICAL EFFECTS

Our results indicate significant bond distortion in nitromethane requires the inclusion of dynamical effects. The lowest energy HOMO-LUMO crossing point found by Manaa and Fried occurs when the nitro group is flipped up out of the CNOO plane. The energy required in this bending mode for the HOMO-LUMO gap to be significantly lowered is about 3 eV. With detonation temperatures around 2000 K in nitromethane, only nonequilibrium processes can be expected to contribute such a large energy to a single bending mode on the molecule. The shock front is a region out of equilibrium where it may be possible for specific vibrational modes of the system to have transiently large populations. At 2000 K the total vibrational energy contained in a single molecule in the solid is about 3.5 eV. Therefore it is at least conceivable that if energy on this scale is contained in a few molecular modes, significant gap lowering could occur via this mechanism. We will see that large changes in the perfect crystal bandgap are more likely to occur via dynamical effects than static effects.

A. Dynamical effects at the shock front

Once the molecules are uniaxially compressed by the shock, they rearrange to their relaxed geometries. It is possible that dynamical bond bending occurs during this rearrangement process. We modeled this process for a rapid shock compression along the *c* axis by doing constant energy *ab initio* molecular dynamics starting with a unit cell with the molecules translated toward each other. The unit cell was also strained 0.2 along the *c* axis to reproduce the uniaxial strain associated with a roughly 13 GPa detonation wave. A 1 fs time step was used with a Verlet algorithm for integration of the equations of motion through about 270 fs. The internal temperature of the molecules was initially at $T=0$, with no vibrational energy. The bandgap started at 0.6 eV below the unstrained crystal bandgap and immediately increased. It did not dip below this value for the remainder of

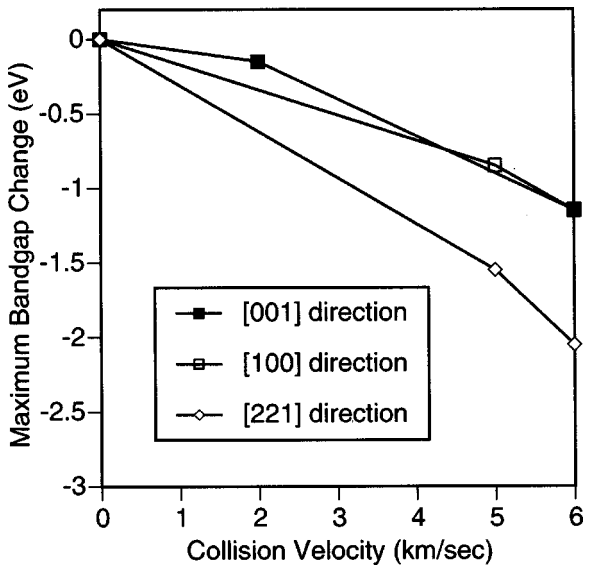

FIG. 13. Maximum bandgap change attained during intermolecular collisions along nearest-neighbor directions in the crystal. Bandgaps are plotted relative to the unstrained crystal bandgap.

the simulation, which is consistent with the minimal bond distortion observed during the rearrangement.

The solid phase molecules exist in a face-centered cubic lattice, with 12 nearest-neighbor molecules. Two neighbors are in the [001] and $[00\bar{1}]$ lattice directions, two are along the [100] and $[\bar{1}00]$ directions, and the remaining eight are along the $[22\bar{1}]$, $[\bar{2}2\bar{1}]$, $[2\bar{2}\bar{1}]$, $[\bar{2}\bar{2}\bar{1}]$, $[22\bar{1}]$, $[\bar{2}2\bar{1}]$, $[2\bar{2}\bar{1}]$, and $[\bar{2}\bar{2}\bar{1}]$ directions. The latter eight nearest neighbors lie along four directions in the crystal which can be shown identical using the four group operations of the $P2_12_12_1$ symmetry. The periodicity of molecular orientations along these directions is four. It is two along the [001] lattice direction, and one along the [100] lattice direction.

By accounting for these symmetries and periodicities, we have done *ab initio* molecular-dynamics simulations of the molecular collisions associated with shock wave propagation along all nearest-neighbor directions in the crystal. This was realized by colliding molecules along the three unique nearest-neighbor directions. Collisions along the [100] and [221] lattice directions were accomplished using an eight molecule supercell with the length of the *a* axis doubled.

Detonation shock waves in nitromethane propagate around 6 km/s, with average atomic (particle) velocities of roughly 2 km/sec.[34] The molecular collision velocities at the shock front depend on the width of the front. This width can be as large as hundreds of molecules in crystals with defects and vacancies, or as short as a few molecules in perfect crystals. We expect the larger molecular collision velocities to be about 2 km/s, which roughly corresponds to the particle velocity. However, molecular collision velocities near the shock velocity are not inconceivable in special cases.

Collisions along all three directions were calculated for collision velocities between 2 and 6 km/s (between 0.02 and 0.06 Å/fs). A 1 fs time step was used for the 2 km/s calculations and 0.5 fs was used for the higher collision velocities. All simulations were run for around 100 fs. The internal temperature of the molecules was initially at $T=0$, with no vibrational energy.

The maximum observed changes in the HOMO-LUMO gaps as a function of collision velocity are given in Fig. 13. This gap minimum was obtained near the peak of the collision in all cases. Figure 13 indicates that the bandgap can be significantly affected at higher collision velocities, but it is still too large for a significant thermal population of excited states to exist.

Little bond bending or stretching was observed in the 2 km/s collision, although some vibrational energy was deposited into the molecular modes. The 5 and 6 km/s collisions showed large amounts of energy being transferred into the CN stretching and methyl rotation degrees of freedom. CN stretching vibrational amplitudes were around 15% after these collisions. The 6 km/s collision along the [100] axis was also done using a GGA spin-polarized exchange-correlation functional.[16] Results obtained were identical to the non-spin-polarized exchange-correlation functional results.

A molecular collision of 10 km/s along the *c* direction was also considered. This collision resulted in immediate rupture of the CN bond. The formation of new species lowered the bandgap 1.4 eV. At the larger collision energies, energy sufficient for bond breaking may be directly channeled into bond-breaking modes. This eliminates the need for a fast excited state decomposition mechanism.

B. Crystal shearing along a slip plane

For shock pressures greater than a few GPa, plastic deformation mechanisms can play a role in the energy transfer from the shock to molecular degrees of freedom. When a system is placed under uniaxial strain, it can plastically deform along slip planes to achieve a hydrostatic stress state. The presence of crystal defects can facilitate this strain relaxation mechanism. Dick *et al.*, have suggested that localized slip along sterically hindered slip planes in the crystal causes molecular bond distortion.[35]

Dick has proposed that detonation in nitromethane is most easily initiated when shocked along directions which require slip along sterically hindered slip planes to relieve the uniaxial stress.[36] As an exemplary sterically hindered slip system, we have considered slip along the (102) plane in the $[\bar{2}01]$ direction, which can be active for relief of uniaxial strain along the [001] direction. Figure 14 shows a view down this slip plane. The $[\bar{2}01]$ direction is into the page, and shearing is accomplished by moving the top and bottom planes directly into and out of the page.

Ab initio molecular dynamics of slip along the (102) plane in the $[\bar{2}01]$ direction were done with an eight molecule supercell with the *a* lattice vector doubled for proper boundary conditions. The *c* axis was strained 0.2 and molecules relaxed. The molecules on opposite sides of the (102) plane were given velocities of 0.03 Å/fs in opposite directions along the $[\bar{2}01]$ axis. This velocity, which is near the shock velocity, is probably larger than might actually occur during slip, but it should accentuate dynamical effects and molecular distortion that occurs during slip. The periodicity of the simulation resulted in single-molecule planes traveling in alternately opposite directions. The simulation was run for 160 fs with a time step of 1 fs. The molecules were initially at $T=0$, with no vibrational energy.

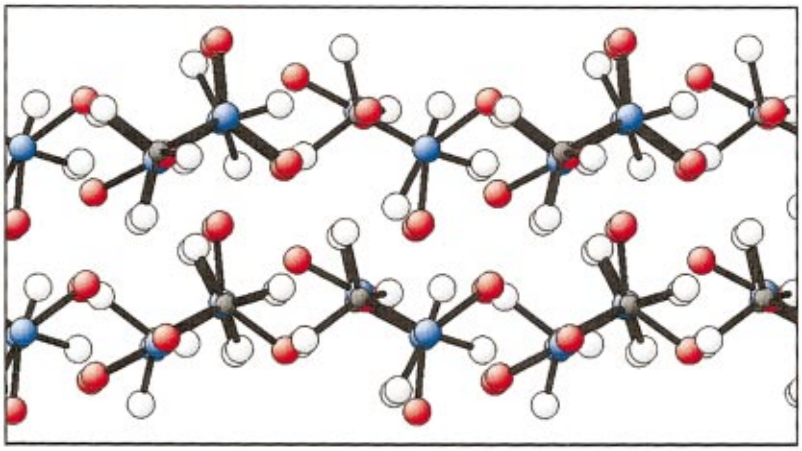

FIG. 14. (Color) A view in the $[\bar{2}01]$ direction along the (102) shearing plane. Shearing is accomplished by the bottom and top planes moving directly into and out of the page.

The coherent motion of the molecules was dispersed after about 50 fs after making close to half of a lattice translation in the $[\bar{2}01]$ direction. After this point the system appeared to be transforming to a liquid state. After 140 fs, molecular CN bonds began to break. A HOMO-LUMO gap dropped 1.6 eV at its lowest in the time observed. This gap lowering is of similar magnitude to the lowering for the nearest-neighbor molecular collisions of the same 6 km/s velocity. The HOMO-LUMO gaps appeared to gradually decrease as the energy from translational motion of the molecules was transferred into the molecular vibrational modes. Some bond bending was observed, but no significant bending of the nitro group out of its plane was observed. Bond bending during the shearing process seems to have been largely avoided through the rotation of the methyl group. Stresses that might have resulted in bond bending in more rigid molecules were relaxed by rotation of the CN bond axis. This particular molecular mode was observed to be the recipient of a significant amount of the shearing energy.

V. DISCUSSION

The work of Manaa and Fried suggests extreme molecular distortions are required to close the HOMO-LUMO gap in nitromethane. However, our results indicate the intermolecular interactions in nitromethane are probably too weak to allow for such significant covalent bond distortion within the molecules under static conditions.

If bandgap closure does occur, it is most likely to be the result of dynamical effects that may occur around crystal defects or during shearing of the molecular crystal. The HOMO-LUMO gap decreases observed at high velocities in the dynamical simulations were much more significant than the bandgap decreases for the perfect crystal under realistic static conditions. These dynamical bandgap changes were comparable in magnitude to the molecular defect bandgap changes for large values of uniaxial strain. Perhaps dynamical effects which involve high velocity collisions between the nitro groups of defect molecules are one of the most likely sources of electronic excitations.

The work of Manaa and Fried suggests roughly 3 eV must be channeled into the CNOO bending mode for the HOMO-LUMO gap to significantly decrease. With temperatures associated with detonation in the 0.2 eV range, this can only occur in regions far from equilibrium where energy from the shock has good coupling into this mode. It may, however, be possible for molecular decomposition to occur before such extreme energies are possessed in any single molecular degree of freedom. For example, an energy of 3 eV in the CN stretching mode will result in dissociation of the methyl and nitro groups.[22]

Some speculation may be made about the role of electronic excited states in the detonation of other high explosives like TATB and TNT. These molecules are larger than nitromethane and may have fundamentally different electronic structures. If the HOMO and LUMO states are localized on the nitro groups, as in nitromethane, then we would not expect significant bandgap lowering to occur under compression or around defects. Larger molecules may, however, be more susceptible to bond bending during shearing processes due to the lack of a single freely rotating methyl group which adjusts to relieve molecular stress. One might generally expect the slip planes of crystals of larger molecules to be more sterically hindered than nitromethane, which could increase the likelyhood of bond bending. However, larger molecules have more bonds to relax applied stresses, which might lower the chances of any single bond being excessively stressed. In light of these observations, it is not clear how to rigorously extrapolate the nitromethane results to larger molecules. However, the similarly weak intermolecular interactions in these materials under normal conditions sheds some degree of doubt on the likelihood of significant bandgap lowering under shock loading.

VI. SUMMARY

We have observed in this work that under the conditions of hydrostatic stress, uniaxial strain, and shear strain associated with shock loading in a detonation wave, the bandgap of crystalline nitromethane and nitromethane with molecular defects and vacancies does not decrease enough for a significant thermal population of molecular excited states. Under these conditions, the molecules rearrange such that no significant molecular geometric distortion occurs. This is facilitated by the nearly free rotation of the molecule along the CN bond axis, which adjusts to minimize stress on the molecule. The localization of the HOMO and LUMO states on the nitro group also plays a role in this result. We also expect little geometric distortion and bandgap lowering to occur around larger defects and vacancies for these reasons.

We have also modeled the molecular collisions at shock fronts and during the shearing of the crystal. It was determined that if significant bandgap lowering occurs, it is most likely to occur via dynamical effects. However, molecular collision velocities in excess of 6 km/s appear to be required to produce a significant thermal population of molecular excited states. The nearly free rotation of the methyl group plays a key role in relaxing stresses on the molecule during these dynamical simulations.

The small methyl group rotation barrier and the localized nature of the HOMO and LUMO states of nitromethane appear to be the biggest factors in keeping the bandgap relatively large during shock conditions. For these reasons, the extension of these results to larger explosive molecules like TATB and TNT is not clear. The possibility of electronic excitation in these materials certainly deserves careful investigation.

ACKNOWLEDGMENTS

We wish to thank Riad Manaa for helpful discussions and calculations in support of this work. We also thank Nikolaj Moll for helpful discussions. Evan Reed acknowledges support from the Department of Defense NDSEG. Some of the research in this paper was performed under the auspices of the U.S. Department of Energy by the University of California Lawrence Livermore National Laboratory under Contract No. W-7405-Eng-48 and the Office of Naval Research Contract No. N0001-94-1-0591.

*Author to whom correspondence should be addressed. Electronic mail: evan@mit.edu

[1] A. Tokmakoff, M. D. Fayer, and D. D. Dlott, J. Phys. Chem. **97**, 1901 (1993).
[2] J. J. Dick, R. N. Mulford, W. J. Spencer, D. R. Pettit, E. Garcia, and D. C. Shaw, J. Appl. Phys. **70**, 3572 (1991).
[3] V. K. Jindal and D. D. Dlott, J. Appl. Phys. **83**, 5203 (1998).
[4] K. L. McNesby and C. S. Coffey, J. Phys. Chem. B **101**, 3097 (1997).
[5] C. S. Coffee, Phys. Rev. B **24**, 6984 (1981).
[6] L. E. Fried and A. J. Ruggiero, J. Phys. Chem. **98**, 9786 (1994).
[7] F. Williams, Adv. Chem. Phys. **21**, 289 (1971).
[8] A. N. Dremin, V. Y. Klimenko, O. N. Davidove, and T. A. Zoludeva, in *The Ninth Symposium* (International) on Detonation (OCNR, Arlington, 1989).
[9] J. Sharma, B. C. Beard, and M. Chaykovsky, J. Phys. Chem. **95**, 1209 (1991).
[10] J. J. Gilman, Philos. Mag. B **71**, 1957 (1995).
[11] For a review, see F. Siringo, R. Pucci, and N. H. March, High Press. Res. **2**, 109 (1989).
[12] M. M. Kuklja and A. B. Kunz, J. Appl. Phys. **86**, 4428 (1999).
[13] Y. Baryam and J. D. Joannopoulos, Phys. Rev. Lett. **52**, 1129 (1984).
[14] M. R. Manaa and L. E. Fried, J. Phys. Chem. A **103**, 9349 (1999).
[15] J. P. Perdew, in *Electronic Structure of Solids '91*, edited by P. Ziesche and H. Eschrig (Akademie-Verlag, Berlin, 1991).
[16] J. P. Perdew, K. Burke, and M. Ernzerhof, Phys. Rev. Lett. **77**, 3865 (1996).
[17] N. Troullier and J. L. Martins, Phys. Rev. B **43**, 1993 (1991).
[18] D. Vanderbilt, Phys. Rev. B **41**, 7892 (1990).
[19] O. H. Nielsen and R. M. Martin, Phys. Rev. B **32**, 3792 (1985).
[20] S. F. Trevino, E. Prince, and C. R. Hubbard, J. Chem. Phys. **73**, 2996 (1980).
[21] S. F. Trevino and W. H. Rymes, J. Chem. Phys. **73**, 3001 (1980).
[22] M. R. Manaa and L. E. Fried, J. Phys. Chem. A **103**, 9349 (1999).
[23] W. M. Ficker, O. A. Mosher, and A. Kuppermann, Chem. Phys. Lett. **60**, 518 (1979).
[24] I. N. Remediakis and E. Kaxiras, Phys. Rev. B **59**, 5536 (1999).
[25] Dionisios Margetis (private communication).
[26] H. Chacham, X. Zhu, and S. G. Louie, Phys. Rev. B **46**, 6688 (1992).
[27] M. S. Hybertsen and S. G. Louie, Phys. Rev. Lett. **55**, 1418 (1985); Phys. Rev. B **34**, 5390 (1986).
[28] D. T. Cromer, R. R. Ryan, and D. Schiferl, J. Phys. Chem. **89**, 2315 (1985).
[29] S. Courtecuisse, F. Cansell, D. Fabre, and J. P. Petitet, J. Chem. Phys. **102**, 968 (1995).
[30] Riad Manaa (private communication).
[31] S. Courtecuisse, F. Cansell, D. Fabre, and J. P. Petitet, J. Chem. Phys. **108**, 7350 (1998).
[32] E. H. Younk and A. B. Kunz, Int. J. Quantum Chem. **63**, 615 (1997).
[33] M. M. Kuklja, E. V. Stefanovich, and A. B. Kunz, J. Chem. Phys. **112**, 3417 (2000).
[34] R. A. Graham, J. Phys. Chem. **83**, 3048 (1979).
[35] J. J. Dick, R. N. Mulford, W. J. Spencer, D. R. Pettit, E. Garcia, and D. C. Shaw, J. Appl. Phys. **70**, 3572 (1991).
[36] J. J. Dick, J. Phys. Chem. **97**, 6193 (1993).
[37] M. E. Tuckerman and M. L. Klein, Chem. Phys. Lett. **283**, 147 (1998).